

COMPUTATION OF TURBULENT NATURAL CONVECTION FLOWS WITH THE ELLIPTIC-BLENDING SECOND-MOMENT CLOSURE

Seok-Ki Choi and Seong-O Kim

Fast Reactor Development Division,
Korea Atomic Energy Research Institute
150-1 Deokjin-dong, Yuseong-gu, Daejeon, 305-353, Korea
skchoi@kaeri.re.kr and sokim@kaeri.re.kr

ABSTRACT

This paper presents the numerical results of natural convection flows using the elliptic-blending second-moment closure. First, the performance of the elliptic-blending model is investigated through application to the natural convection of air in a rectangular cavity with an aspect ratio of 1:5. Second, the treatment of turbulent heat fluxes for calculation of the turbulent natural convection is investigated. Three different cases for treating the turbulent heat fluxes are considered. Those are the generalized gradient diffusion hypothesis (GGDH), the algebraic flux model (AFM) and the differential flux model (DFM). Comparisons are made for a natural convection in an 1:5 cavity and the natural convection in a square cavity with conducting top and bottom walls. Then, the computational results of a turbulent Rayleigh-Benard convection is presented. The elliptic-blending model together with the algebraic flux treatment of the turbulent heat fluxes result in the most accurate solution without invoking numerical stability. It is observed that the GGDH treatment results in a very poor solution for a stratified flow. The elliptic-blending model with the algebraic flux model predicts well the important parameters of the Rayleigh-Benard convection.

INTRODUCTION

An accurate prediction of a natural convection is very important for investigating the fluid flow and heat transfer in various nuclear engineering applications such as a reactor vessel auxiliary cooling system in a liquid metal reactor and the thermal stratification in an upper plenum of a liquid metal reactor during a scram condition. Despite its importance in practical engineering problems, it is still difficult to solve accurately the turbulent natural convection by the current turbulence models. Most work in the literature employs the RANS (Reynolds Averaged Navier-Stokes) equation approach even though a few DNS (Direct Numerical Simulation) and LES (Large Eddy Simulation) solutions exist for low Rayleigh number flows. Several works in the literature used different turbulent models or different treatment of turbulent heat fluxes. However, there does not exist a unique turbulence model that performs better than the other models. In the present study the performances of the elliptic-blending second-moment closure are tested for a simple shear flow, a thermally stratified flow and the Rayleigh-Benard convection. The

computed results are compared with those of the other turbulence models, the LES results and the experimental data.

THE ELLIPTIC-BLENDING TURBULENCE MODEL

Manceau and Hanjalic (2002) developed an elliptic-blending model. The model has been further modified by Thielen et al. (2005). The governing equations for the elliptic-blending model are as follows;

$$\frac{D}{Dt}(\rho) = 0 \tag{1}$$

$$\frac{D}{Dt}(\rho U_i) = -\frac{\partial p}{\partial x_i} + \frac{\partial}{\partial x_j} \left(\mu \frac{\partial U_i}{\partial x_j} - \overline{\rho u_i u_j} \right) - \rho \beta g_i (\Theta - \Theta_{ref}) \tag{2}$$

$$\frac{D}{Dt}(\rho \Theta) = \frac{\partial}{\partial x_j} \left(\frac{\mu}{Pr} \frac{\partial \Theta}{\partial x_j} - \overline{\rho \theta u_j} \right) \tag{3}$$

$$\begin{aligned} \frac{D}{Dt}(\overline{\rho u_i u_j}) = \frac{\partial}{\partial x_k} & \left[\left(\mu \delta_{kl} + C_s \rho \overline{u_k u_l} T \right) \frac{\partial \overline{u_i u_j}}{\partial x_l} \right] \\ & + \rho (P_{ij} + G_{ij} + \Phi_{ij} - \varepsilon_{ij}) \end{aligned} \tag{4}$$

$$\begin{aligned} \frac{D}{Dt}(\rho \varepsilon) = \frac{\partial}{\partial x_k} & \left[\left(\mu \delta_{kl} + C_\varepsilon \rho \overline{u_k u_l} T \right) \frac{\partial \varepsilon}{\partial x_l} \right] \\ & + \rho \frac{(C_{\varepsilon 1}(P_k + G_k) - C_{\varepsilon 2} \varepsilon)}{T} \end{aligned} \tag{5}$$

$$\begin{aligned} \frac{D}{Dt}(\overline{\rho \theta^2}) = \frac{\partial}{\partial x_k} & \left[\left(\frac{\mu}{Pr} \delta_{kl} + C_{\theta\theta} \rho \overline{u_k u_l} T \right) \frac{\partial \overline{\theta^2}}{\partial x_l} \right] \\ & + \rho \left(2P_\theta - R \frac{\varepsilon}{k} \overline{\theta^2} \right) \end{aligned} \tag{6}$$

$$\alpha - L^2 \frac{\partial^2 \alpha}{\partial x_j \partial x_j} = 1 \tag{7}$$

where

$$P_{ij} = -\overline{u_i u_k} \frac{\partial U_j}{\partial x_k} - \overline{u_j u_k} \frac{\partial U_i}{\partial x_k}, G_{ij} = -g_i \overline{\beta u_j \theta} - g_j \overline{\beta u_i \theta} \tag{8}$$

$$P_\theta = -\overline{u_k \theta} \frac{\partial \Theta}{\partial x_k} \tag{9}$$

$$\Phi_{ij} = (1 - \alpha^2) \Phi_{ij}^w + \alpha^2 \Phi_{ij}^h \tag{10}$$

$$\begin{aligned} \Phi_{ij}^h = & \left(C_1 + C_2 \frac{P_k}{\varepsilon} \right) \varepsilon A_{ij} + C_3 k S_{ij} + C_4 k \left(A_{ik} S_{jk} + A_{jk} S_{ik} - \frac{2}{3} \delta_{ij} A_{kl} S_{kl} \right) \\ & + C_5 k \left(A_{ik} \Omega_{jk} + A_{jk} \Omega_{ik} \right) - C_6 \left(G_{ij} - \frac{2}{3} G_K \delta_{ij} \right) \end{aligned} \tag{11}$$

$$\Phi_{ij}^w = -5 \frac{\varepsilon}{k} \left(\overline{u_i u_k n_j n_k} + \overline{u_j u_k n_i n_k} - \frac{1}{2} \overline{u_k u_l n_k n_l} (n_i n_j + \delta_{ij}) \right) \quad (12)$$

$$\varepsilon_{ij} = (1 - \alpha^2) \frac{u_i u_j}{k} \varepsilon + \frac{2}{3} \alpha^2 \varepsilon \delta_{ij} \quad (13)$$

$$n = \frac{\nabla \alpha}{\|\nabla \alpha\|}, \quad A_{ij} = \frac{u_i u_j}{k} - \frac{2}{3} \delta_{ij} \quad (14)$$

$$S_{ij} = \frac{1}{2} \left(\frac{\partial U_i}{\partial x_j} + \frac{\partial U_j}{\partial x_i} \right), \quad \Omega_{ij} = \frac{1}{2} \left(\frac{\partial U_i}{\partial x_j} - \frac{\partial U_j}{\partial x_i} \right) \quad (15)$$

$$T = \max \left(\frac{k}{\varepsilon}, C_T \left(\frac{\nu}{\varepsilon} \right)^{1/2} \right), \quad L = C_L \max \left(\frac{k^{3/2}}{\varepsilon}, C_\eta \left(\frac{\nu^3}{\varepsilon} \right)^{1/4} \right) \quad (16)$$

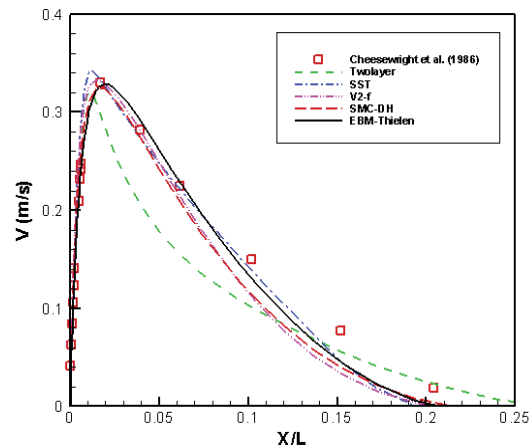
RESULTS AND DISCUSSION

Natural Convection in a 1:5 Rectangular Cavity

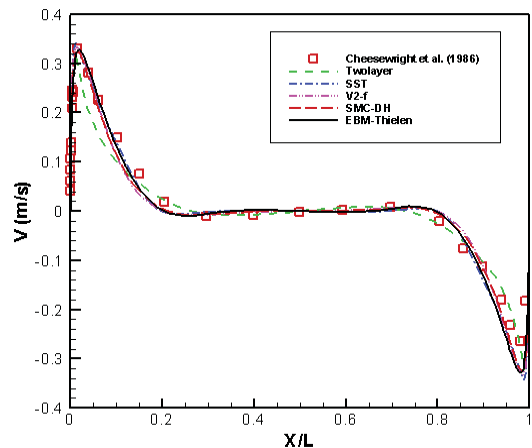
The test problem considered in this section is the natural convection of air in a rectangular cavity with an aspect ratio of 1:5. The Rayleigh number based on the height of the cavity is $Ra = 4.3 \times 10^{10}$. King (1989) has carried out extensive measurements for this problem. For this problem, the relative performances between the elliptic-blending model (EBM) and the two-layer model, the shear stress transport model (SST), the V2-f model and the second moment differential stress and flux model (SMC-DH) are investigated. We first compare the predicted results with the measured data for the vertical mean velocity at the mid-height ($y/H=0.5$) of the cavity. As shown in the Fig.1, the agreement between the measured data and the predictions by the SST, V2-f, SMC-DH and EBM models are fairly good although there is a small difference. The prediction by the two-layer model is significantly different from the measured data. This model produces a laminar-like solution in the near wall region.

Fig.2 shows the profiles of the predicted turbulent heat fluxes, $\overline{\theta v}$ and $\overline{\theta u}$, at the mid-plane ($y/H=0.5$) of the cavity with the measured data. It is noted that the vertical turbulent heat flux vector $\overline{\theta v}$ plays a very important role in the dynamics of the turbulent kinetic energy in the buoyant turbulent flows and it influences directly the overall prediction of all the quantities. The AFM (algebraic flux model) used in the present study for the two-layer, SST and V2-f models, contains all the temperature and mean velocity gradients together with the correlation between the gravity vector and temperature variance. All the models predict well the vertical turbulent heat flux and this is due to the fact that the constants in the AFM have been adjusted to predict accurately the vertical turbulent heat flux for each model. The V2-f and SMC-DH models slightly under-predict the vertical turbulent heat flux $\overline{\theta v}$ near the hot wall and the peak regions of $\overline{\theta v}$ are skewed a little toward the center region as shown in Fig. 4-(b). The two-layer model predicts well the vertical turbulent heat flux near the hot wall region and the peak regions are skewed to the hot wall, but the shape of the predicted profile is a little thin when compared with the other predictions. The EBM model under-predicts the vertical turbulent heat flux, however, the

shape of the predicted vertical turbulent heat flux by this model follows the trend of the experimental data. Fig.4-(a) shows that the SMC-PH and EBM models predict very accurately the horizontal turbulent heat flux $\overline{\theta u}$, while the other models over-predict it severely. This fact shows that the GGDH which is used with the EBM model predicts the turbulent heat flux well when the turbulent stresses are predicted accurately.



(a) Near the hot wall



(b) Total view

Fig.1 Mean vertical velocity profiles at $y/H=0.5$

Fig.3 shows the comparison of the predicted results with the measured data for the local Nusselt number at the hot wall. The V2-f model and EBM predict accurately the local Nusselt number at the hot wall, and the transition phenomenon at the lower portion of the hot wall is also predicted well. The SMC-DH model predicts the local Nusselt number at the hot wall well, however, it does not predict the laminar to turbulent transition observed in the experimental data. The two-layer and SST models predict the local Nusselt number at the hot wall very poorly and they also do not predict the transition phenomenon. The EBM predicts best the mean vertical velocity component and the local Nusselt number at the hot wall.

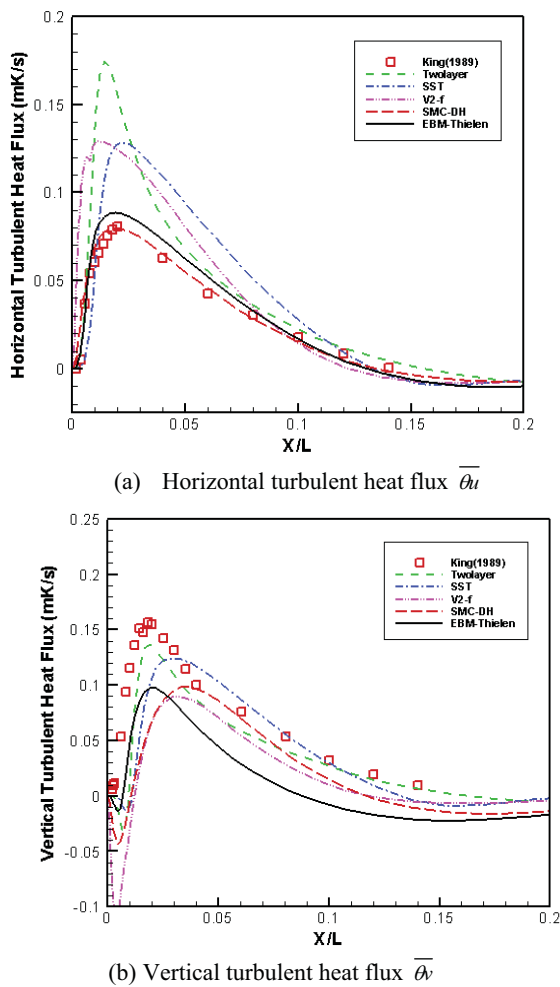


Fig.2 Turbulent heat fluxes profiles at $y/H=0.5$

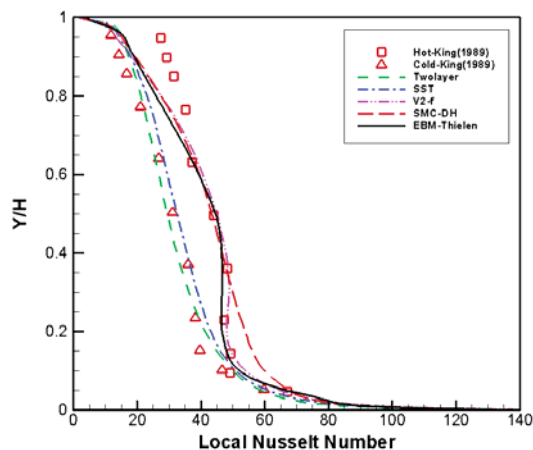


Fig.3 Local Nusselt number profiles along hot wall

Fig.4 shows the comparison of the predicted results with the measured data for the wall shear stress at the hot wall reported in King (1989). We observe that V2-f model predicts the peak value of the wall shear stress at the hot wall well, but it over-predicts the wall shear stress after the peak region. The trend of the prediction of the wall shear

stress by the SMC-DH model is nearly the same as that by the V2-f model and the SMC-DH model slightly under-predicts the peak value of the wall shear stress. The trend of the prediction by the two-layer and SST model is different from that by the V2-f and SMC-DH models. We can observe that even the V2-f and SMC-DH models do not predict the laminar to turbulent transition well at the hot wall observed in the experimental data. They predict a smooth transition. It is noted that the measurement of the velocity components near the bottom wall is more accurate than that near the top wall due to insufficient insulation at the top wall. The EBM model predicts the wall shear stress best.

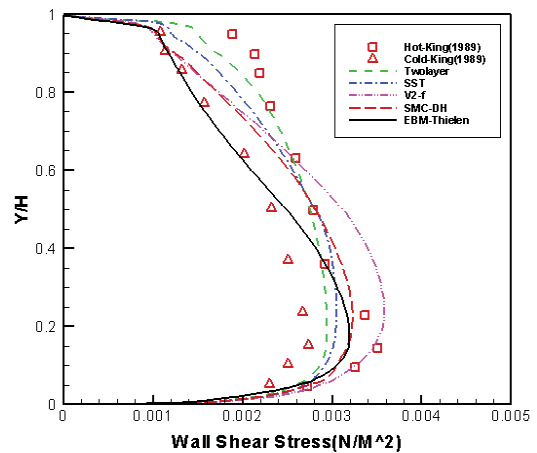


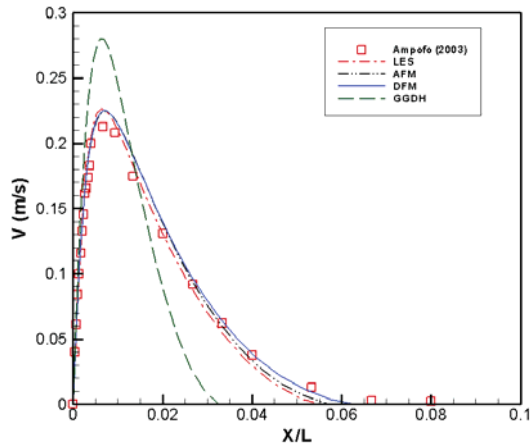
Fig.4 Wall shear stress distribution along the vertical wall

Natural Convection in a Square Cavity with Conducting Walls

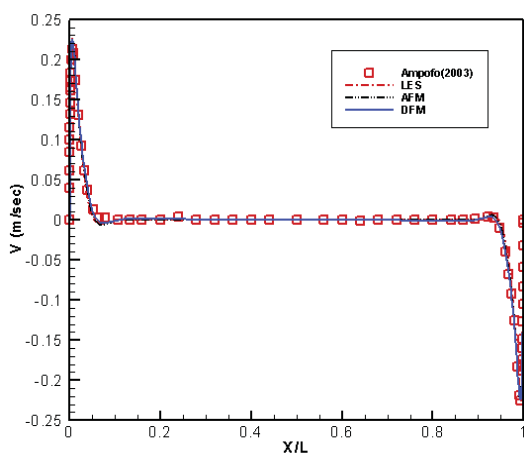
The second test problem is a natural convection of air in a square cavity with two isothermal side walls and two conducting walls at the top and bottom. The Rayleigh number based on the height of the cavity is $Ra = 1.58 \times 10^9$ and the Prandtl number is $Pr = 0.71$. The detailed experimental data is tabulated in Ampofo and Karayinnis (2003). The LES solution by Peng and Davidson (2001) is available for this flow and it is compared with the present predictions. In this study the effect of different treatment of turbulent heat flux is also studied. Three types of treatment of turbulent heat flux, GGDH (General Gradient Diffusion Hypothesis), AFM (Algebraic Flux Model) and DFM (Differential Flux Model), are considered.

Fig. 5 shows the comparisons of the predicted results with the measured data for the vertical velocity component at a mid-height ($y/H=0.5$) of the cavity. As shown in the figure, the agreement between the measured data and the predictions by the AFM and DFM models is very good and follows the trend of the measured data. However, we can observe that the solution by the GGDH model looks like laminar solution and deviates much from the experimental data. Choi and Kim (2006) predicts accurate solutions for a simple shear dominant flow within the 1:5 rectangular cavity using the GGDH model, however, this model predicts a very poor solution or invokes a numerical

oscillation when applied to a flow with a relatively strong stratification like the present problem. We can observe that the predictions by the AFM and DFM turbulence models are as good as the LES solution.



(a) Near the hot wall



(b) Total view

Fig. 5 Mean vertical velocity profiles at $y/H=0.5$

Fig.6 show the comparisons of the predicted results with the measured data for the Reynolds shear stress at a vertical mid-plane of the cavity ($y/H=0.5$). Fig.6 shows that the predictions by the AFM and DFM agree well with the measured data while the LES severely under-predicts the Reynolds shear stress. It is not understood why the LES calculation by Peng and Davidson (2001) under-predicts the Reynolds shear stress.

Fig.7 shows the predicted results for the local Nusselt number at the hot wall together with the measured data. It is observed that the AFM and DFM slightly over-predict the local Nusselt number at the hot wall, while the LES accurately predict it. It is noted that the predictions of the local Nusselt number at hot wall by the AFM and DFM show a smooth transition which was not observed in the experimental data and LES solution. Although they are not presented here, we also made comparisons for turbulent quantities, such as the vertical velocity fluctuation and the

AFM and DFM predicts fairly well while the LES slightly under-predicts them.

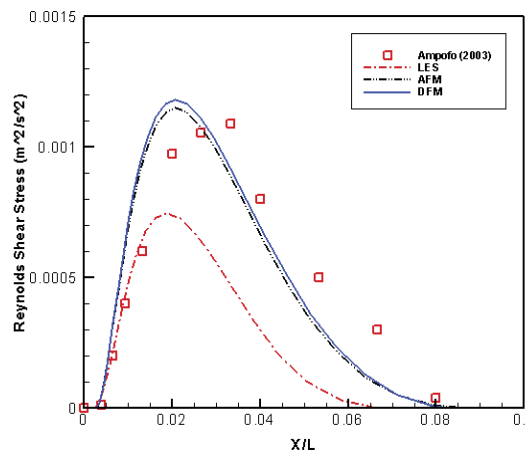
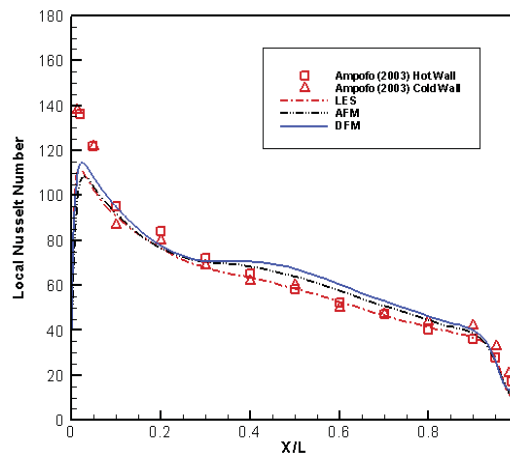
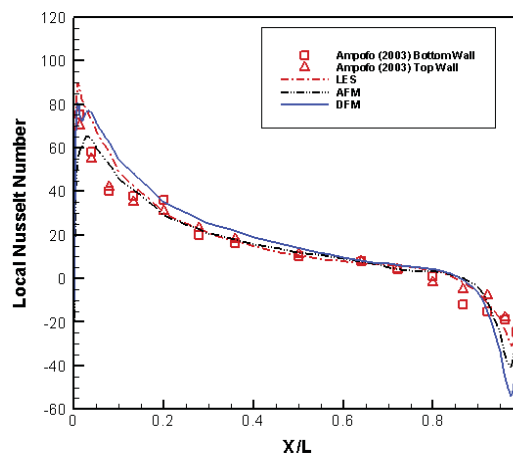


Fig.6 Reynolds shear stress \overline{uv} at $y/H=0.5$



(a) Hot wall



(b) Bottom wall

Fig. 7 Local Nusselt number distributions along the hot and bottom walls

Rayleigh-Benard Natural Convection

As a typical case of a Rayleigh-Benard convection, we consider a natural convection within an enclosure of a 8:1 aspect ratio where the bottom wall is heated and the upper wall is cooled. A symmetry condition is imposed at the lateral boundaries to mimic the infinite horizontal boundaries. The 82 non-uniform grids are generated in the vertical direction and the smallest grid size near the walls is $\Delta y/H = 4 \times 10^{-4}$ where H is the vertical distance between two horizontal walls. In the lateral direction 127 uniform grids are generated. Calculations are performed for six different Rayleigh numbers, 2×10^6 , 10^7 , 4×10^7 , 10^8 , 5×10^8 and 10^9 .

Fig.8 shows the predicted velocity vectors and streamlines for $Ra = 10^7$ and $Ra = 10^9$ respectively. We can observe that the number of rolls is nine when $Ra = 10^7$ and it is seven when $Ra = 10^9$. One roll exists at the center and the other rolls are symmetric with respect to the center roll, and the number of rolls is an odd number for both cases. In our test calculations, the formation of the roll structures depends on the numerical method, initial and boundary conditions and the Rayleigh number. Like in the previous calculations, the size of the roll increases with an increase of the Rayleigh number.

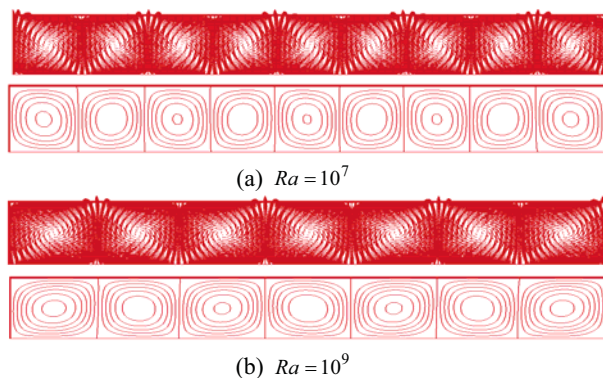


Fig.8 Velocity vectors and streamlines

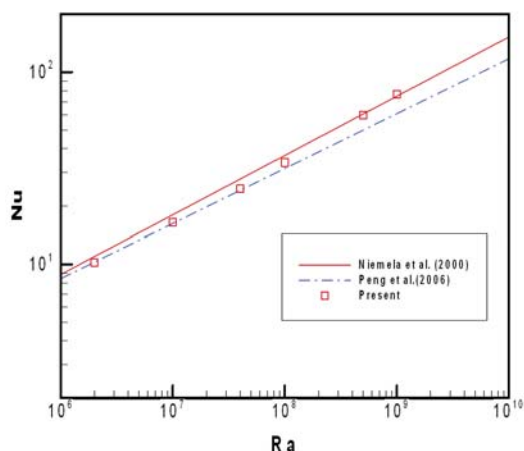


Fig.9 The predicted overall Nusselt number versus Rayleigh number with the LES results and the experimental correlation

It is very difficult to compare our results with other DNS, LES and experimental data since no detailed experimental or DNS data are available for a higher Rayleigh number region. The only way for a validation of the computation can be made by comparing the long term averaged Nu numbers with experimental correlations. However, many contradictions exist regarding the Nusselt number versus Rayleigh and Prandtl numbers relation ($Nu \approx cRa^a Pr^b$). Many correlations by DNS, LES and experiments have been proposed in the past and the results of these studies are summarized well in Kenjeres (1998) and Kenjeres and Hanjalic (2000). In the earlier studies the relation $Nu \approx Ra^{1/3}$ was proposed, however, Wu and Libchaber (1992) and another Chicago group claimed that such a correlation only works for a low-Rayleigh number region. This scaling region ($Ra \leq 4 \times 10^7$) is called a ‘soft’ convective turbulence region and a higher Rayleigh number region ($Ra \geq 4 \times 10^7$) is called a ‘hard’ convective turbulence region. Most of the previous authors developed a single correlation that covers ‘soft’ and ‘hard’ convective turbulence regions.

Fig. 9 shows the present results for the overall Nusselt number versus Rayleigh number together with the correlation by the LES results from Peng et al. (2006) ($Nu = 0.162Ra^{0.286}$) and the experimental correlation by Niemela et al. (2000) ($Nu = 0.124Ra^{0.309}$). This figure shows that our results follow with the correlation by Peng et al. (2006) in the ‘soft’ convective turbulence region ($Ra \leq 4 \times 10^7$) well, and at the transition point ($Ra \approx 4 \times 10^7$), the simulation results begin to deviate from the correlation by Peng et al. (2006), and after a certain transition region around $Ra \approx 10^8$, it follows the correlation by Niemela et al. (2000) at the ‘hard’ convective turbulence region ($10^8 \leq Ra \leq 10^9$). Within the present author’s knowledge, nobody has reported a numerical simulation or experimental correlation that shows this trend. The fine grid ($256 \times 128 \times 256$) LES solution by Kenjeres and Hanjalic (2006) matches very well with the present results for Rayleigh numbers ranging $10^8 \leq Ra \leq 10^9$. It is unfortunate that they did not carry out calculations for Rayleigh number less than $Ra \approx 10^7$. One may claim that the correlation by Niemela et al. (2000) can be used for the whole Rayleigh number region ($10^6 \leq Ra \leq 10^9$) for an engineering purpose since the maximum percentage difference between two correlations in the ‘soft’ convective turbulence region is around 10%. However, the difference between the two correlations becomes grave in the ‘hard’ convective turbulence region ($10^8 \leq Ra \leq 10^9$). It is worth while mentioning that the two-dimensional prediction by Kenjeres and Hanjalic (2000) follows the experimental correlation by Niemela et al.(2000), even in the ‘soft’ convective turbulence region. They used a modified version of the low-Reynolds number $k-\epsilon$ model by Launder and Sharma (1974). As shown in Fig.8 the flow involves more impinging regions in the ‘soft’ convective turbulence region and it is well known that the $k-\epsilon$ turbulence model

predicts an excessively high turbulence kinetic energy in an impinging stagnation region. It is our conjecture that their over-prediction of the Nusselt number in the 'soft' convective turbulence region may be due to this stagnation anomaly of the $k-\varepsilon$ turbulence model. When the Rayleigh number becomes higher, the impinging region becomes smaller. Then, the effect of the stagnation anomaly of the $k-\varepsilon$ turbulence model becomes smaller, and thus, their results closely match with our results. It is noted that the elliptic-blending second-moment closure used in the present study predicts the flow in the impinging stagnation region very well (Thielen et al., 2005).

CONCLUSIONS

(1) The elliptic-blending model performs best for a simple shear flow in an 1:5 rectangular cavity. When one considers the fact that the wall related parameters are not present in the EBM model and its performance is as good as or better than the usual second-moment closure, the use of the EBM is highly recommended.

(2) The AFM and DFM perform similarly for a natural convection flow in a square cavity involving thermal stratification. The GGDH model predicts a very poor solution or invokes a numerical oscillation when applied to a flow with a relatively strong thermal stratification.

(3) The EBM predicts fairly well the Rayleigh-Benard convection. The predicted overall Nusselt number follows Peng et al. (2006) at the 'soft' convective turbulence region ($Ra \leq 4 \times 10^7$) and it follows Niemela et al. (2000) at the 'hard' convective turbulence region ($10^8 \leq Ra \leq 10^9$).

REFERENCES

- Ampofo, F. and Karayiannis, T. G., 2003, "Experimental Benchmark Data for Turbulent Natural Convection in an Air Filled Square Cavity", *Int. J. Heat Mass Transfer*, Vol. 46, pp. 3551-3572.
- Choi, S. K. and Kim, S. O., 2006, "Computation of a Turbulent Natural Convection in a Rectangular Cavity with the Elliptic-Blending Second-Moment Closure", *Int. Comm. Heat Mass transfer*, Vol. 33, pp. 1217-1224.
- Kenjeres, S., 1998, "*Numerical Modeling of Complex Buoyancy-Driven Flows*", Ph.D Thesis, Delft University of Technology, The Netherlands.
- Kenjeres, S. and Hanjalic, K., 2000, "Convective Rolls and Heat Transfer in Finite-Length Rayleigh-Benard Convection: A Two-Dimensional Numerical Study", *Phys. Rev. E*, Vol. 62, pp.7987-7998.
- Kenjeres, S. and Hanjalic, K., 2006, "LES, T-RANS and Hybrid Simulations of Thermal Convection at High Ra Numbers", *Int. J. Heat Fluid Flow*, Vol. 27, pp. 800-810.
- King, K. V., 1989, *Turbulent Natural Convection in Rectangular Air Cavities*, Ph.D Thesis, Queen Mary College, University of London, UK..
- Lauder, B. E. and Sharma, B. I., 1974, "Application of the Energy Dissipation Model of Turbulence to the

Calculation of Near Spinning Disc, *Lett. in Heat and Mass Transfer*, Vol. 1, pp.131-138.

Manceau, R., and Hanjalic, K., 2002, "Elliptic Blending Model: a New Near-Wall Reynolds-Stress Turbulence Closure", *Phys. Fluids*, Vol. 14, pp. 744-754.

Niemela, J. J., Skrbek, L., Sreenivasan, K. R. and Donnelly, R.J., 2000, "Turbulent Convection at Very High Rayleigh Numbers", *Nature*, Vol. 404, pp.837-840.

Peng, S. H., Hanjalic, K., and Davidson, L., 2000, "Large-eddy Simulation and Deduced Scaling Analysis of Rayleigh-Benard Convection up to $Ra=10^9$ ", *J. Turbulence*, Vol. 7, pp. 1-29.

Peng, S. H., Davidson, L., 2001, "Large Eddy Simulation of Turbulent Buoyant Flow in a Confined Cavity", *Int. J. Heat Fluid Flow*, Vol. 22, pp.323-331.

Thielen, L., Hanjalic, K., Jonker, H. and Manceau, R., 2005, "Prediction of Flow and Heat Transfer in Multiple Impinging Jets with an Elliptic-Blending Second-Moment Closure", *Int. J. Heat Mass Transfer*, Vol. 48, pp.1583-1598.

Wu, X. Z. and Libchaber, A., 1992, "Scaling Relation in Thermal Turbulence", *Phys. Rev. A*, Vol. 40, pp.842-845.